



Modelling of rainfall-induced landslide: a threshold-based approach

Abhishek Prakash Paswan¹ · A.k. Shrivastava¹

Received: 19 August 2021 / Accepted: 31 March 2022 / Published online: 15 April 2022
© Saudi Society for Geosciences 2022

Abstract

Landslides during the rainy season are a usual phenomenon resulting in loss of human, animal, and property and obstructing the transportation facilities of the area. Modelling is an established tool for the reliable, efficient, and feasible study of landslide mechanisms. Modelling is done by simulating the material properties and boundary conditions for an existing failed slope. In the present study, an area subjected to the recurrence of landslides during the rainy season has been selected to study the mechanism that triggers landslides. After extensive fieldwork and computation of hydro-mechanical parameters through a series of laboratory experiments, a semi-similar material physical model test was conducted to study the sliding mechanism and its crucial factor. Furthermore, numerical modelling has also been done using GeoStudio to analyze the seepage and slope stability parameters to verify and compare the results to assess the suitability of this study. An artificial rainfall simulator is designed and developed to simulate the quantity and intensity of rain to study the failure mechanism and the threshold level of rainfall that causes the triggering of landslides. The physical model slope failed at 80 mm threshold rainfall depth at a 30 mm/h fixed intensity. Numerical analysis results show that the slope remains stable with a safety factor of 1.23 before the rainfall. Still, after simulating the rainfall condition for the physical model test, the slope fails at the same rainfall intensity and depth with an approximately similar failure plane with a safety factor of 0.626, indicating that rainfall is the major affecting parameter that generally initiates the landslide. This study also proves the suitability and feasibility of numerical modelling to analyze different slopes, providing scientific guidance for monitoring and early warning so that preventive measures can be taken to reduce its effect.

Keywords Rainfall-induced landslides · Slope failure · Physical modelling · Numerical modelling · Threshold rainfall depth · Early warning system.

Introduction

Landslides are common and deadly occurrences across the world, posing a threat to life, property, agricultural lands, and so to the engineering buildings (Parkash 2011). The Himalayan slope is more susceptible to landslides than landslides occurred around the globe as the Himalayan Mountain is a new fold mountain compared to others (Gupta et al. 2016). The delicate nature of soil formation of Himalayan

areas, along with rainfall conditions and numerous phylogenies actions, has made the region prone to landslides (Singh et al., 2018). Figure 1 shows the landslide hazard zonation map of India and Himachal Pradesh. Several recurring landslides occur every rainy season, which causes tremendous loss of life and property in the study area, due to which life and survival become challenging for days (Kanungo and Sharma 2014). Many studies reveal that the frequency of landslides increased due to rainfall percolation (Iverson 2000; Dahal 2012). The frictional resistance criterion determines the strength of a slope in an unsaturated condition; however, as water infiltrates through soil pores, negative pore pressure, also known as matric suction, aids in increasing slope stability; however, excessive infiltration causes the soil to become saturated, resulting in a loss of frictional strength, resulting in slope failure (Yang et al. 2015; Kristo et al. 2017; Lin and Zhong 2019; Cai et al. 2020; Zhao 2021). Figure 2 explains the sequential stages

Responsible Editor: Biswajeet Pradhan.

✉ Abhishek Prakash Paswan
abhishek_mt2k16@dtu.ac.in

A.k. Shrivastava
aksrivastava@dce.ac.in

¹ Department of Civil Engineering, Delhi Technological University, New Delhi, India

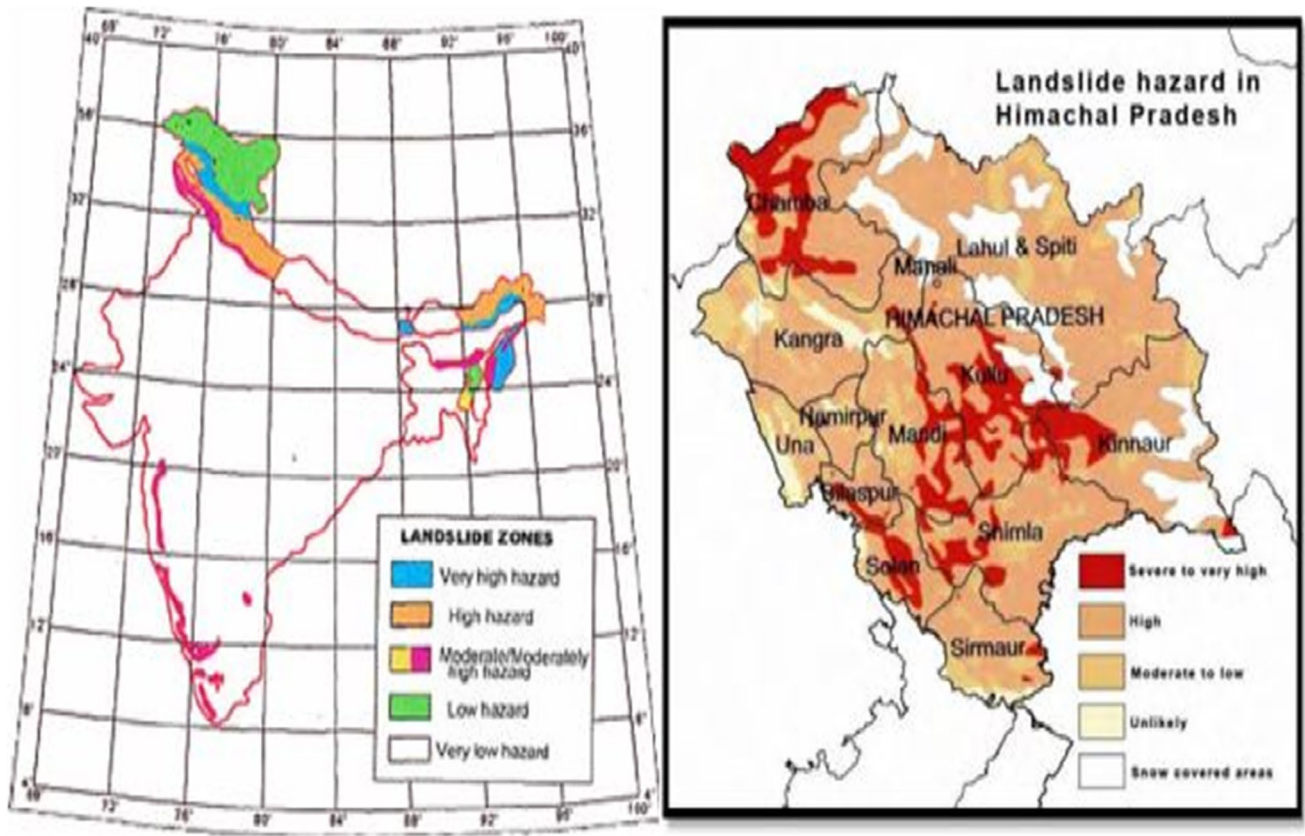
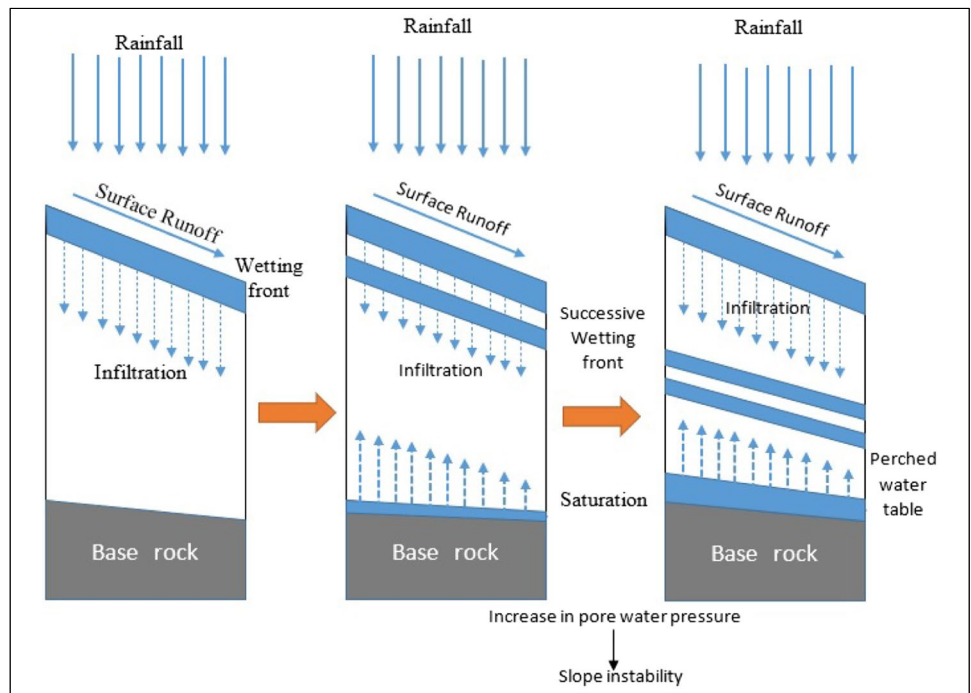


Fig. 1 Landslide hazard in Himachal Pradesh. HPSDMA Himachal Pradesh, 2011

Fig. 2 A sequential schematic of landslide initiation (Kuriakose et al. 2009)



for rainfall infiltration and accumulation between the soil layers. Rainfall usually triggers slope failures. The water gets infiltrated between soil layers, and water accumulation occurs, reducing the soil layer's shear strength. Because the soil on the surface becomes saturated, the water makes its approach right down to the lower layers. With excessive rainfall, deep percolation occurs between the rock and soil layer, which accumulates and creates the fluid zone near the surface, reducing the shear strength and leading to the landslide (Kuriakose et al. 2009).

After extensive studies, many researchers concluded that rainfall is the most common cause of landslides in the Indian Himalayas and rainfall acts as the initiation factor to slope failure (Dikshit et al. 2020a). There are mainly three methods used extensively to analyze the stability and failure slip surface of the landslide: physical modelling, numerical modelling, or mathematical modelling. With the delicate and unpredictable nature of rainfall-induced landslides, it is really tough to analyze the actual failure mechanism only with a mathematical or numerical model (Li et al. 2016). So physical modelling proved to be an effective method for analysis of failure mechanisms and generation of thresholds that can be further used for prediction and warning systems. Li et al. (2016) investigated the failure cause of a landslide in China using a physical model test based on a similar material theory. The landslide initiation factors and start-up conditions are proposed, which can be used for prevention and forecasting purposes. To examine the triggering mechanisms of landslides caused by rainfall, a series of small-scale physical modelling tests are conducted in a geotechnical drum centrifuge to investigate the potential failure causes for a full-scale landslide experiment (Askarinejad, et al., 2012; Matziaris et al. 2015). Only a few researchers have done a comparative study of physical and numerical modelling to validate the results of the study (Josifovski et al. 2019; Xie et al. 2021). Many researchers have used the numerical analysis method to analyze the stability and failure slip surfaces under different boundary conditions (Singh et al., 2018; Zhang et al. 2019; Luo et al. 2021; Paswan and Shrivastava, 2022a, b). Although there are various techniques available for numerical analysis, GeoStudio is widely used for the analysis of rainfall-induced slope instability because of its feasibility and efficiency (Acharya et al. 2016; Jeong et al. 2017; Lin and Zhong 2019; Zhao 2021). The threshold can also be derived using other methods like empirical methods (Guzzetti et al. 2008; Abraham et al. 2020c), probabilistic methods (Dikshit et al. 2018, 2020b; Abraham et al. 2020a), mathematical model (Peres et al. 2018), and algorithm base model (Abraham et al. 2022) but the drawback with these methods is that they need long-term temporal data to generate precise thresholds and warnings, leading to a high number of false predictions for any particular site. With the evolution of electronic components and methods, there

are several instruments available for real-time monitoring of a particular slope based on tilt angle and pore water pressure (Uchimura et al. 2015; Abraham et al. 2020b). Electronic instruments can generate extremely effective warnings with a very low probability of false alarm, but their high cost, the requirement for specialized installation, and high maintenance requirements make this method unsuitable for every vulnerable slope. Remote sensing techniques are also widely in use to assess the landslide hazard: Panchal and Shrivastava (2022) performed landslide hazard assessment using analytic hierarchy process (AHP) in Indian Himalayan region and also done a comparative study for landslide susceptibility assessment using Shannon's entropy and AHP models (Panchal and Shrivastava 2021).

An extensive literature review based on the analysis and prediction methods for rainfall-induced landslides reveals a high increase in landslide events in the Indian Himalayan region during the monsoon season. Still, very few studies on rainfall-induced landslides have been performed in the Indian Himalayan region to analyze and visualize failure mechanisms. Only a few comparison studies have been conducted to compare the outcomes of numerical methods with those of physical modelling tests for validation purposes.

In this study, a recurring slope from the Himalayan region is selected, and scale-based modelling is done in the laboratory according to similar theories. This study is performed to investigate the failure patterns using the physical modelling method generating a rainfall threshold, and numerical analysis using GeoStudio has been done for comparison and validation of both approaches. This threshold can provide scientific guidance for monitoring and early warning of rainfall-induced landslides so that preventive measures can be taken to reduce its effect. The specific objectives of this study are to prepare a physical model in the laboratory to analyze a rainfall-induced landslide failure pattern by physical modelling, to develop a self-made rainfall simulator for the desired rainfall, to analyze the behavior of pore water pressure during rainfall, to analyze the behavior and nature of seepage through soil pores, to understand the role of soil properties in landslide failure, and to compare and analyze the failure mechanism by numerical modelling using GeoStudio software with physical modelling results.

Study area

The study location is on NH-5 in Jhakri town of Shimla district in Himachal Pradesh, India (Fig. 3). The study area is covered under the topo sheet no. 53/E11 (1973) by the SOI. NH-5 is a major national highway-connecting corridor for Shimla districts to other areas of Himachal Pradesh. There are two hydroelectric projects of 1500 MW and 343 MW capacity operated by Satluj Jal Vidyut Nigam (SJVN) Ltd

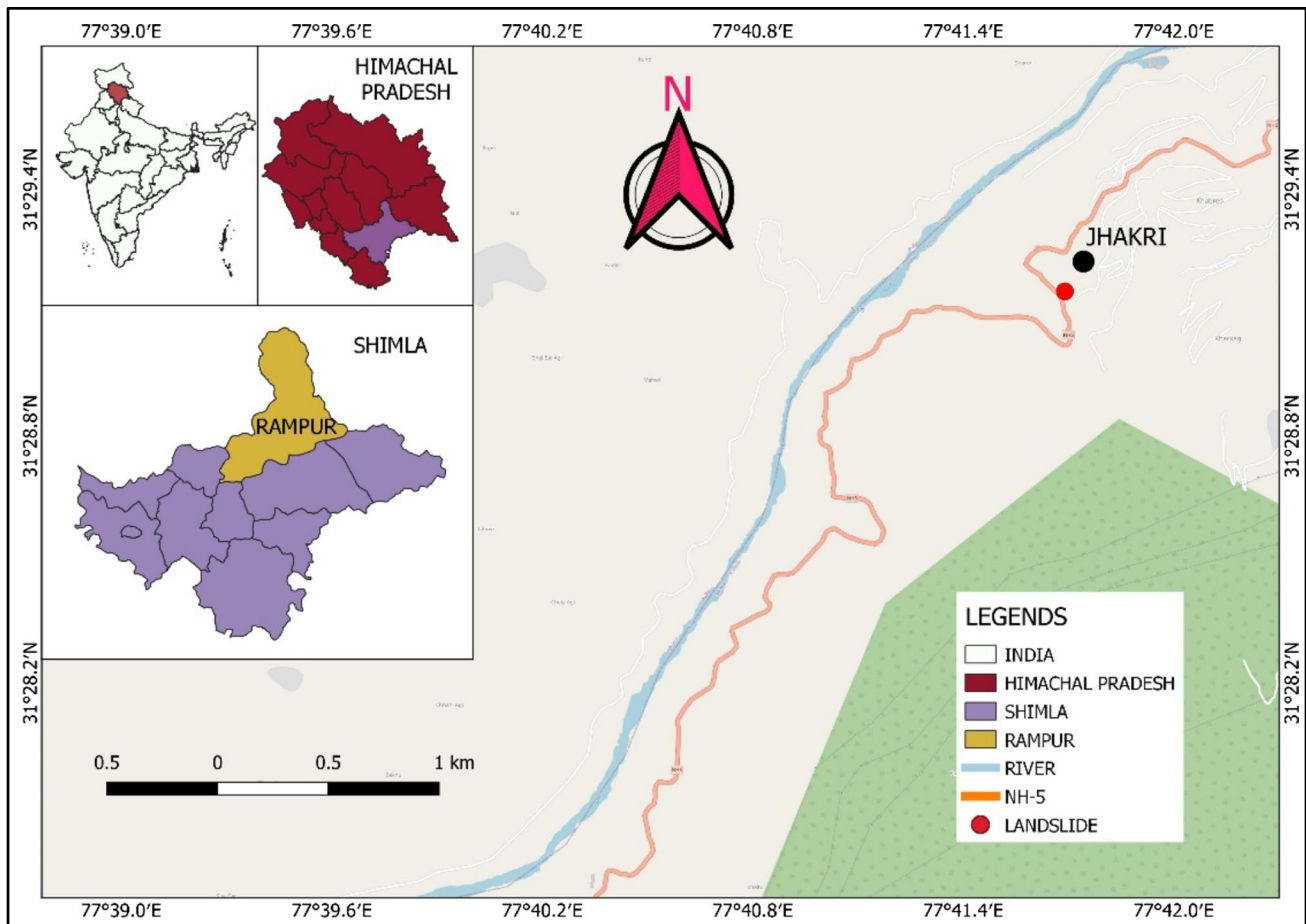


Fig. 3 Location map of the study area situated in Rampur district of Shimla, Himachal Pradesh, India

in this area (Singh et al., 2018). The location is situated near the Sutlej River that is the rainfall catchment basin of the study area. Jhakri area is highly affected by a rainfall-induced landslide near the NH-5 (HPSDMA Himachal Pradesh, 2011).

Description of the slope

The studied slope is near a tributary of river Sutlej. The digital elevation model of Rampur is shown in Fig. 4a, while Fig. 4b shows the elevation profile of the study area. The slope has a height of 55.3 m, with a slope angle of 35° that has been observed. The slope material contains loose aggregate deposits composing highly weathered rock particles. The soil material is non-uniform in grain size containing various sizes of rock and stones. Surface runoff was prominent, which can be justified by the presence of erosional gullies and slope surface. The Jhakri area has experienced many devastating landslides in the past. The sloping section of the Jhakri area along NH-5 has a wide history of failure. It

infrequently obstructs the road because of the mass of debris and rolling boulders (Geological Survey of India).

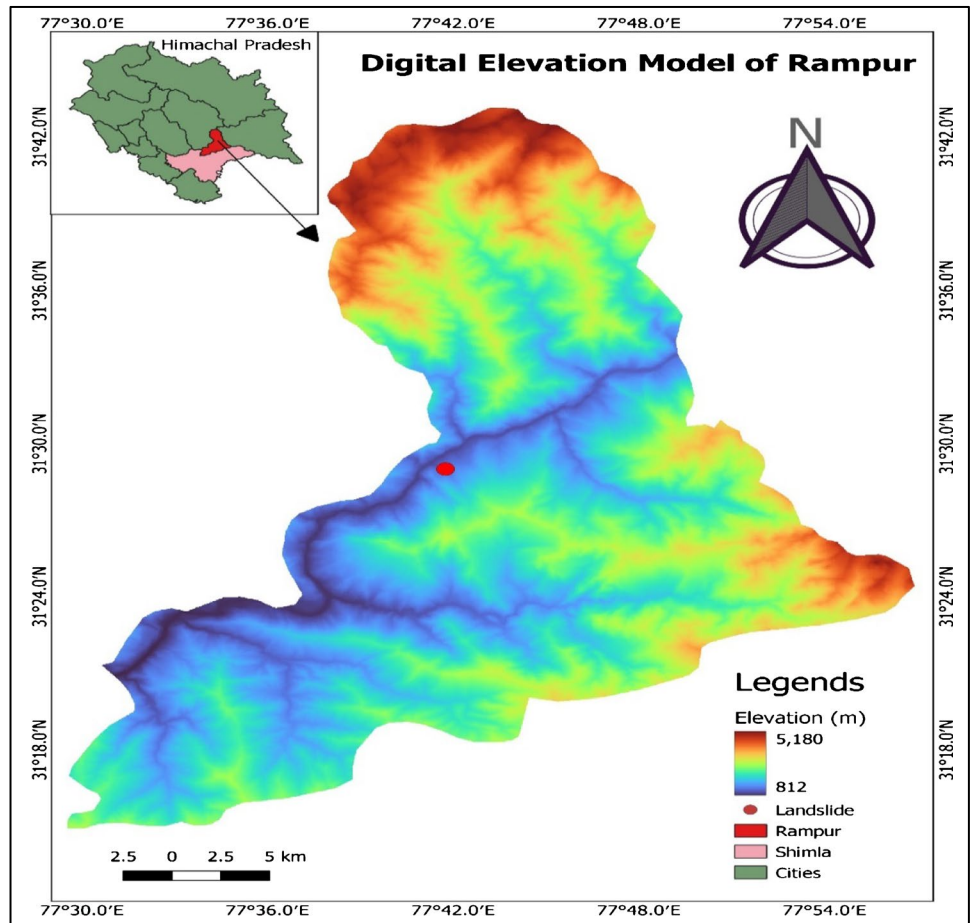
Geotechnical investigation of slope material

To determine the material properties of the failure slope, soil samples were collected from different places of the slope at the study area. By performing particle size distribution test in laboratory according to BIS standards (IS:2720 (Part 4):1985), the result shows that the material consists of 60% sand, 36% silt, and 4% clay. Some fractions of stones were also available in a non-homogeneous way, and the gradation of slope material comes as non-uniform as there was a wide range of particles present. The soil is classified as silty sand in nature.

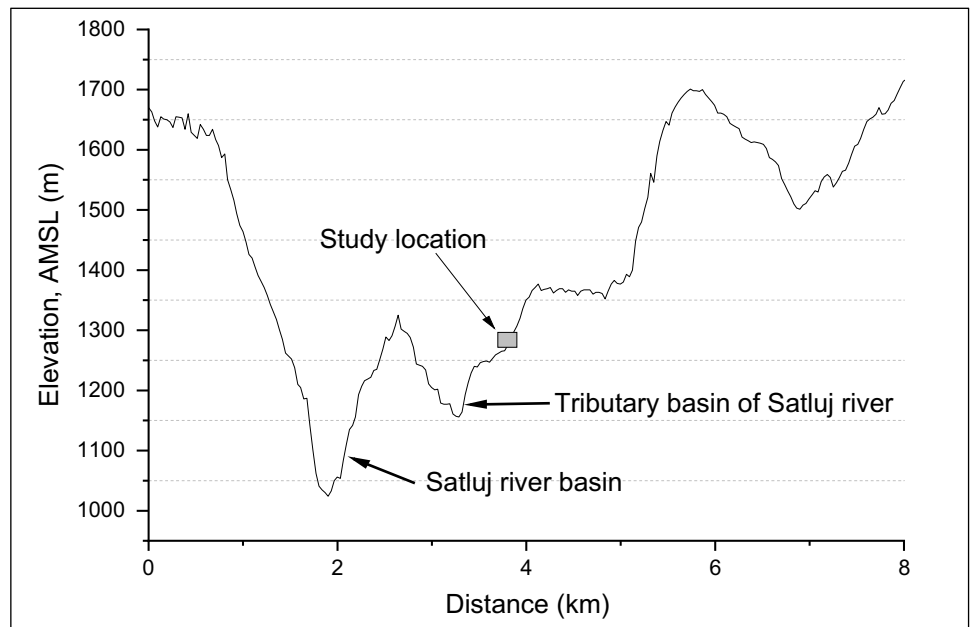
Rainfall characteristics

As stated above, the study area comes under the catchment area of Sutlej Valley. Rainfall in this area is because of the S-W monsoon due to the orographic mechanism. The S-W

Fig. 4 a DEM of Rampur, Shimla, and b elevation profile of the study area

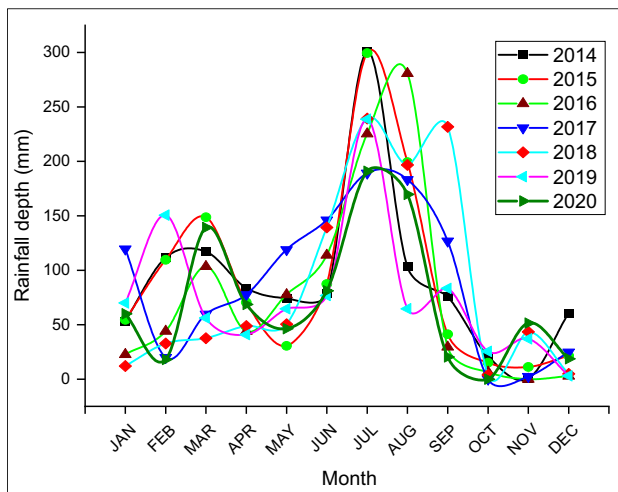


(a)

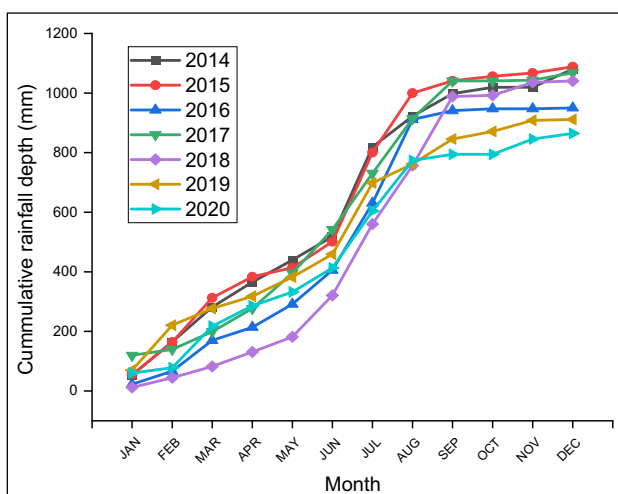


(b)

monsoon appears from June–September along with maximum precipitation depth (HPSDMA 2009). Figure 5a shows the monthly precipitation variation for the Shimla district. The precipitation data for the particular area were taken from the Shimla Regional Center of the Indian Meteorological Department (IMD). By analyzing the monthly rainfall variation for 7 consecutive years, it can be seen that the maximum rainfall received is in between June and July followed by some minor rainfall every month which helps in the development of positive pore water pressure which acts as key factor in initiation of landslide. It explains the reason behind increased number of landslides in monsoonal season and also provides an indication towards the focused study during the monsoonal season.



(a)



(b)

Fig. 5 **a** Monthly precipitation variation and **b** Cumulative rainfall variation

Mechanism of landslide

According to Indian standard code (IS 14496 (Part 2): 1998), slope and geometry, lithology, state of stress, pore pressures, structure, material properties, and boundary conditions all contribute to the landslide mechanism. Because of the high number of landslides that occur in the area during the monsoon season, this research focuses on the characteristics of rainfall that occur when a slope fails. The slope section under investigation has a moderate slope gradient and a semi-circular failure surface. Because of the lower height, the failed section is critically stable in the dry state, but saturation may further reduce the stability. Since the previous segment described how water saturation on the slope exacerbates the problem, rainfall characteristics may provide additional insight into the failure mechanism. As rainwater infiltrates the soil, it activates the shallow failure in four stages: Water movement to the failure zone or bedrock-soil interface zone (interflow, surface flow), loss of soil cohesion or slide, material mobilization, and collapse of the material (Wieczorek 1996). Sharma et al. (2013) have suggested that increased water content from heavy monsoon rains could worsen slope conditions. The diagram (Fig. 2) depicts the progression of shallow landslide initiation in a step-by-step manner. In this case, the rainwater percolation results in the saturation of the interface zone, resulting in the development of a perched water table and the subsequent appearance of successive wetting fronts. Positive pore-water pressure or decreased suction head results in a decrease in soil shear strength and effective stress (Iverson 2000).

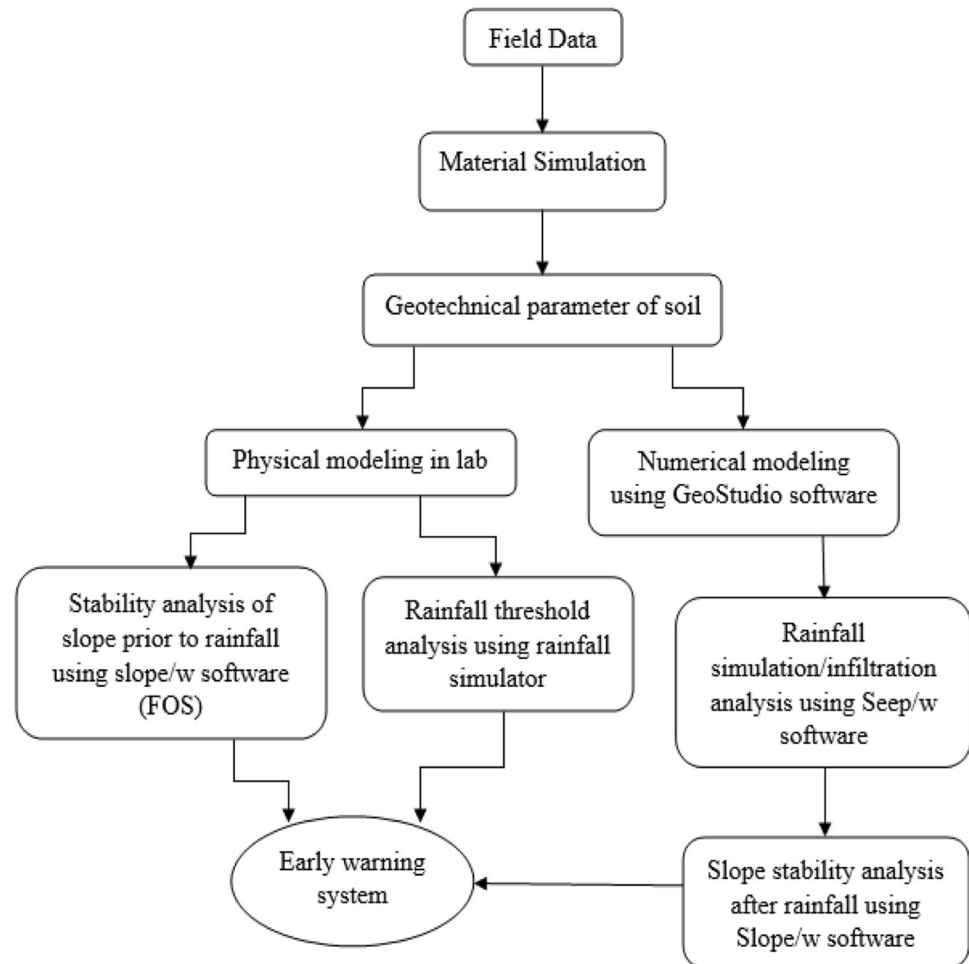
Methodology

In this study, physical modelling has been done in the laboratory to study the mechanism of slope failure in the study area by replicating the field conditions. As it was not feasible to bring that much soil from the location, so material simulation has been done using parent soil geotechnical properties by similar material theory (Li et al. 2016). Numerical modelling has also been done in this study to verify the results of physical modelling using GeoStudio software (Acharya et al. 2016). Figure 6 shows the Flow chart of the methodology adopted in the present study.

Material similarity and similar condition

A similar theory is used for the indoor model experiment. The experimental set-up and materials are prepared by a similar criterion based on the similar theory. Similarity ratio is adapted accordingly, which is the prototype ratio to model for the parameters: geometric similarity ratio, quality similarity ratio, loading similarity ratio, and boundary

Fig. 6 Flow chart of the methodology adopted in the present study



condition similarity ratio (Skempton 1985; Li et al. 2016; Wong et al. 2017).

The scale-based physical model is mostly used models than any other mechanical model to study the landslide mechanism. A model test used for the study of landslides should have its similarity characteristics, including dead load similarity, slope material similarity, rainfall duration similarity, and boundary condition similarity. These factors are effective parameters in the physical model test used to study the landslide mechanism.

The soil available in the laboratory (DTU soil) constitutes 80% sand, and 20% is fine-grained soil, i.e., silt and clay. The study area constitutes 60% sand and 40% fine-grained soil. So, to meet the similarity condition, sand and clay are added to the DTU soil. As in the study area, there are stones and boulders that are also present in debris material, so we mixed stones and boulders of different sizes to meet up with similarities. By material similarity theory, the similarity ratio of inner friction angle, modulus of elasticity, cohesion, and Poisson's ratio are taken similar to the prototype, as $C_\phi = C_E = C_c = C_\mu = 1$.

Physical modelling

Debris flows are fast-moving landslides that are dangerous to life and property because they move quickly, destroy objects in their paths, and often strike without warning. Debris flows are most common during seasons of heavy rain, and they usually begin on slopes or mountains. Debris flows, also known as mudslides, mudflows, or debris avalanches, are a form of landslide (Abraham et al. 2021). It is tough to explain the mechanism of debris flow landslide, only with a numerical or mathematical model because of sudden failure, complexity, and random behavior (Li et al. 2016). So, the study of slope failure mechanism is done by adopting a physical model test as it is most effective and widely used method to explore the sliding mechanism of soil slices, to investigate the rainfall water movement through the pores, and to analyze the rainfall-induced slope instability, and as an early warning and control of landslides (Askarinejad, et al., 2012; Luo et al. 2015; Li et al. 2016).

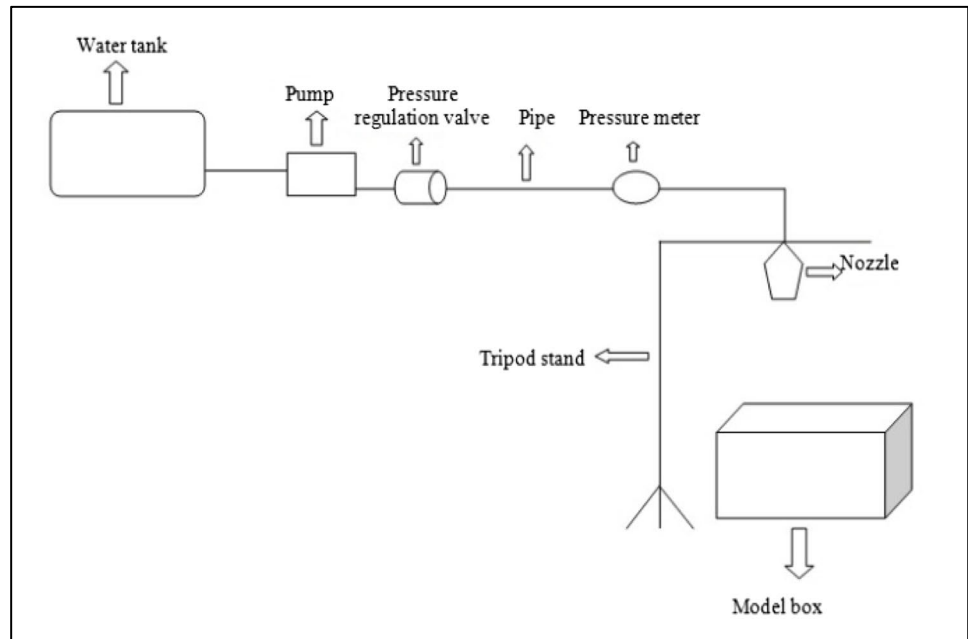
The following assumption has been made while performing the physical modelling. The engineering properties of

parent soil and experimental soil are the same. All the sides are impermeable, ensuring no seepage except the toe drain. The impact factor of rainfall on the slope is negligible as the sprinkler used is not jet type. Rainfall distribution on the slope is uniform. The effect of vegetation has not been considered.

A physical modelling test has been enforced in the study bearing identical engineering properties based on the previous analysis. The essential engineering properties of soil

obtained through similar materials are tested in the laboratory and derived through the dimensional technique. The similar conditions of the physical model experiment were brought in line with the similar theories. The start-up conditions and failure mechanism of the rainfall-induced landslide are studied through the physical model experimental method. Figure 7a shows the schematic diagram of the experimental set-up and Fig. 7b shows the frame type box with soil slope.

Fig. 7 a Schematic diagram of experimental set-up and b frame type model box with soil slope



(a)



(b)

Frame type box

The frame type model is designed using a transparent acrylic sheet of 15 mm thickness with a steel frame for experimental work. The similarity ratio of geometry $C_G = n$. In this test, the geometry scale is taken 1 in 100 as the prototype is large. The experimental platform is a cube tank, which measures 97 cm long, 57 cm wide, and 48.5 cm high. Drain holes are also provided at the toe side to flush the runoff water.

Rainfall simulator

There are two main empirical methods based on precipitation measurement to define its threshold, which is (1) rainfall obtained for a particular event (intensity–duration (ID), total event precipitation (E), precipitation event–duration (ED), and precipitation event–intensity (EI) thresholds) (Guzzetti et al. 2008) and (2) antecedent precipitation activity (Guzzetti et al. 2008) which is outlined as the threshold amount of rainfall that would cause slope failure (Iverson 2000; Godt et al. 2009). In this study, three parameters have been considered, (a) intensity of precipitation “ q ,” (b) duration of precipitation “ t ,” and (c) interval of precipitation. The rainfall duration and interval each vary with the time factor. The relationship between the intensity of rainfall “ q ” and the total rainfall “ Q ” is as follows:

$$q = \frac{Q}{t} \quad (1)$$

Figure 5b shows the cumulative rainfall variation for 7 successive years which defines the maximum rainfall depth for the particular year which helps in deciding the threshold rainfall depth for landslide. For this study, the rainfall depth is kept to 10 mm in each rainfall till the failure occurs, and variable interval of 15 min, 30 min, 45 min, and 60 min is kept for next successive rainfalls to make moisture infiltrate properly. An artificial rainfall simulator is designed including a water tank, submersible pump, control valve, and raindrop nozzle to generate the desired rainfall.

To generate the desired rainfall depth with varying pressure, a pump is installed in the rainfall simulator. The discharge capacity of the pump is 0.05 l/s, which is 0.18 m³/h. A sluice valve is attached to the rainfall simulator having scales drawn on it to control the flow of water. The hand wheel is rotated to increase or decrease the flow as needed; further marking is done according to experimental need.

For the generation of rainfall, a sprinkler is installed in a rainfall simulator to simulate the rainfall. It has a fixed

opening, so the size of water droplets cannot be changed, which is also a restriction in this modelling. The impact effect of sprinkler was negligible as the rainfall simulator was not jet type. To achieve the desired cumulative rainfall depth, the sprinkler is placed at 12.5 cm height above the slope to make the experiment feasible. The rainfall intensity of 30 mm/h is considered under heavy rainfall conditions. The intensity was constant for this study. Furthermore, the rainfall depth is varied to find out the failure mechanism, pattern, and threshold rainfall depth at which the slope failure occurs because the rainfall data is given in terms of depth by IMD (Indian Meteorological Department), which can be easily understandable for local people.

Numerical modelling

In the present numerical study, a two-dimensional approach is used to investigate the triggering of rainfall-induced landslide for the validation purposes. As it was very tough to generate the real geometry for the failed slope so for getting explicit conclusion, the straight slope is considered following many previous researches (Li et al. 2016; Lin and Zhong 2019; Zhang et al. 2019; Zhao 2021). To implement two-dimensional approach for getting explicit conclusion, following assumptions were made (GEO-SLOPE 2012a, b, c): Slope fails in a single layer as the soil particles are small and compacted. The failure pattern is circular. Maximum failure depth can only be extending to the soil depth. The bottom-most layer underneath the soil mass is assumed to be impermeable; that is, there will be no percolation possible through the soil layer to bedrock. The hydrological and mechanical parameters of soil are the same as the failed soil for saturated and unsaturated cases and the maximum rate of water percolation is equal to soil permeability.

Slope stability analysis has been widely used to deal with complex calculation, investigation, prototype modelling, testing, design, and stability analysis of natural, artificial rock, and soil slopes. The researcher and design engineer typically use the slope stability analysis to assess the safe design of artificial or natural slopes. Slope stability is the resistance of the inclined surface between the layers of soil to failure by sliding or collapsing. The main objectives of slope stability analysis are finding the critical failure section, analyzing potential failure mechanisms, and designing slopes considering safety, reliability, and economics (Zhang et al. 2011; Acharya et al. 2016; Jagodnik 2019).

In this study, the soil slope is analyzed using GeoStudio 2020 software. First, the unsaturated slope is analyzed for its stability using SLOPE/W, which is based on the limit equilibrium method, and then the stability of the slope is analyzed after the rainfall. The rainfall modelling has been done in SEEP/W based on the finite element method,

and then the results generated from SEEP/W have been used in SLOPE/W to check the stability of saturated slope after the rainfall using the Morgenstern and Price method (Morgenstern and Price 1967).

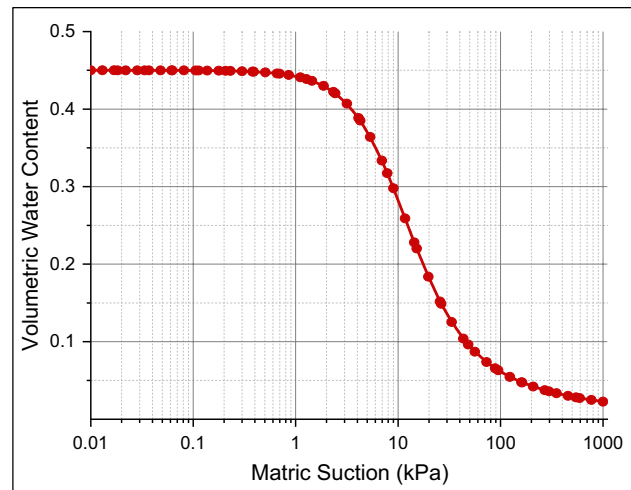
Rainfall infiltration analysis

The SEEP/W based on the 2D finite element method has been used to obtain the pore water pressure generated by the rainfall of desired intensity for the defined material property, slope cross-section, and initial and boundary conditions. It uses a numerical discretization technique to solve Darcy's equation shown in Eq. 2 for unsaturated or saturated slope conditions and runs the following water flow governing equation to compute 2D seepage (Hopkins et al. 1975; Collins and Znidarcic 2004; Harris et al. 2012; Acharya et al. 2016).

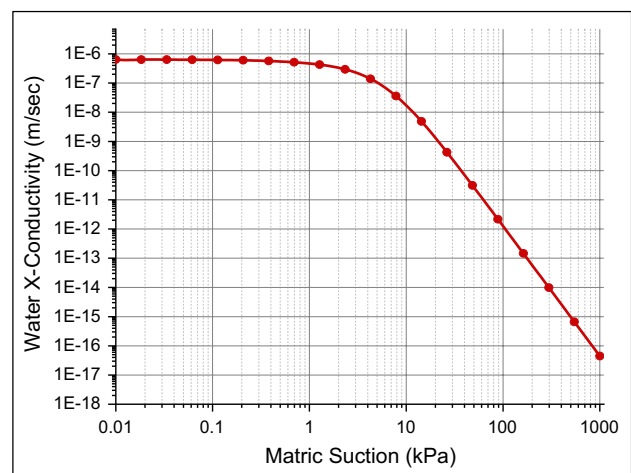
$$\frac{\partial}{\partial x} \left(k_x \frac{\partial H}{\partial x} \right) + \frac{\partial}{\partial y} \left(k_y \frac{\partial H}{\partial y} \right) + q = m_w^2 \gamma_w \frac{\partial H}{\partial t} \quad (2)$$

where “ k_x is used to represent the horizontal x-direction infiltration coefficient, k_y is used to represent the horizontal y-direction infiltration coefficient, H denotes total head of water, q denotes the applied rainfall intensity, m_w denotes the slope for the SWCC (soil–water characteristic curve), and γ_w denotes the water's unit weight.”

The two main input parameters for this analysis are volumetric water content function (VWCF) shown in Fig. 8a, also widely known as the soil–water characteristic curve (SWCC) function, and hydraulic conductivity function (HCF) shown in Fig. 8b. VWCF shows the relationship between volumetric water content vs. matric suction, and the HCF shows the relationship between water conductivity and matrix function. Matric suction expresses the water-retaining capacity of the soil. The function has been defined using the GeoStudio software with the help of material properties like grain size distribution and the material's hydraulic conductivity. For soils with identical grain-size distributions, the SWCC function was employed, while the HCF function was calculated from the SWCC using the (Fredlund et al. 1994) criteria. The criteria eliminate the requirement for additional prediction approaches to assess residual water content. The SWCC function and the HCF function were combined with the field measurements of saturated water content and soil permeability during the simulation. A limiting suction of -20 kPa was introduced in the analysis as an initial condition to avoid the excessively high negative pore water pressure. The initial water table has been defined along with the impermeable bedrock (Seep; Ltd. 2002;



(a)



(b)

Fig. 8 a Volumetric water content function. b Hydraulic conductivity function

GEO-SLOPE International Ltd 2012b; Harris et al. 2012; Acharya et al. 2016).

Stability analysis

SLOPE/W software, which uses the limit equilibrium method, has been used to examine the slope's stability. Several methods exist for calculating the slope's safety, but the Morgenstern-Price method was used in this investigation. Due to its ability to maintain both force and moment equilibrium, this approach is frequently employed in engineering applications. A relationship between interslice shear (X/E) and normal force (E) is established by the interslice force function $[f(x)]$, where $f(x)$ is the scaling factor. Because it reduces interslice shear at the toe and crest and concentrates shear force in the middle of the sliding mass, the half-sine interslice

force function was used in this study. The slope stability analysis was performed using a modified Mohr–Coulomb soil strength method that also takes into account the variation in shear strength due to matric suction in the soil (GEO-SLOPE 2012a, b, c). The governing equation for this model is given in Eq. 3.

$$\tau = c' + (\sigma_n - u_a) \tan \varphi' + (u_a - u_w) \tan \varphi^b \quad (3)$$

where “ τ denotes the soil’s shear strength, c' denoting the effective value of cohesion strength, $(\sigma_n - u_a)$ denotes the net effective value of normal stress, σ_n denotes the total stress, $(u_a - u_w)$ denotes negative pore water pressure also known as matric suction, u_w denotes the value of pore-water pressure, φ' denotes the friction angle of soil, and φ^b denotes angle between the rate at which shear strength increases in relation to the negative pressure.”

Geometry modelling

Two geometry models have been made for the numerical analysis. One geometric model is for stability analysis before rainfall and the other one is for stability analysis after rainfall analysis. The models have been included with rainfall boundary condition on its slope and zero pressure boundary condition at the toe side of the slope to define the exit point for the water flow.

Results

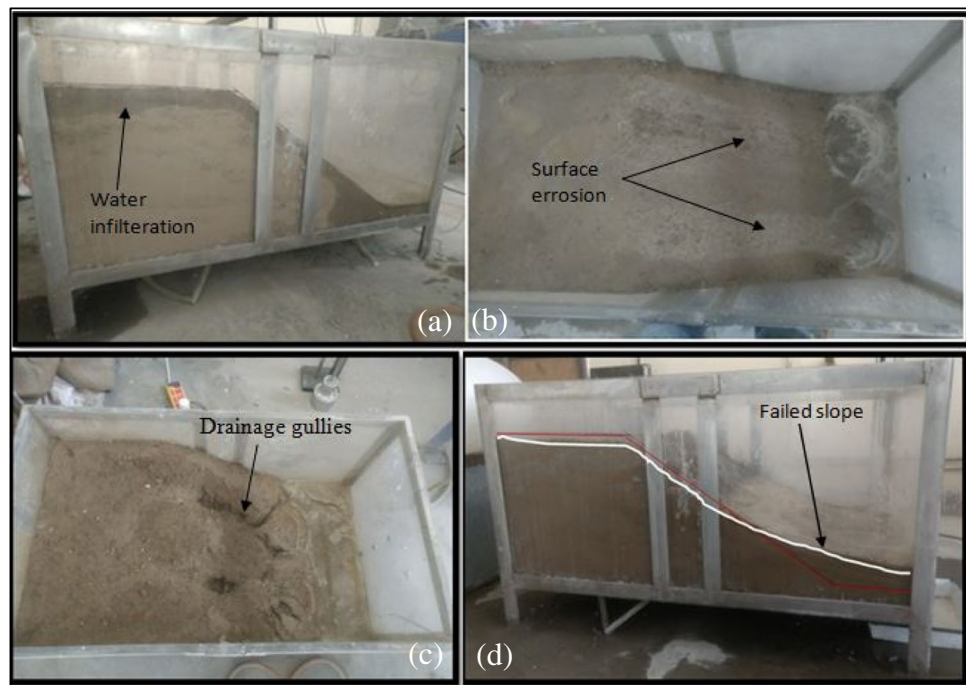
Laboratory test result

The soil taken from the DTU campus named DTU soil is mixed with Yamuna sand and clay to meet the similar condition of parent soil. Laboratory investigation has been done to find the properties of soil for the analysis of slope stability. Different physical and engineering properties of the soil are obtained by conducting different tests according to the Bureau of Indian Standards 2720 (IS:2720 (Part 2) 1973; IS:2720 (Part 3):1980 1980; IS: 2720 (part 12) 1981; IS: 2720 (part 8) 1983; IS: 2720 (part 5) 1985; IS: 2720 (part 17) 1987; BIS:2720 (Part 1) 2006; IS: 2720 (part 7) 2011). The soil was classified as silty sand in nature. The natural water content was 6.7%. Bulk unit weight, dry unit weight, and saturated unit weight were 14 KN/m³, 13.3 KN/m³, and 18.27 KN/m³, respectively. Permeability coefficient was 0.0023 m/h, cohesion 9.5 kPa, and friction angle was 32°.

Physical modelling test result

The rainfall intensity for the adopted slope area, which is 0.6099 m², is fixed to 30 mm/h as a high-intensity rainfall. The effect of rainfall on the slope with 10 mm rainfall depth variation is shown below to visualize the failure pattern of the slope. The images shown in Fig. 9 are clearly describing the progressive stage of a rainfall-induced landslide in the experiment performed. It presents the complete process of

Fig. 9 Effect on the slope for **a, b** 30 mm rainfall, **c** 50 mm rainfall, **d** 80 mm rainfall



occurrence, development, and sliding of the landslide under rainfall. Figure 9a and b indicate that for 30 mm depth of rainfall, water percolation occurs. Due to the high volume of runoff water generated by heavy rain, the effects of weathering and erosion can be seen on the slope face. With continued rainfall of 50 mm depth, the non-uniform vertical settlements can be seen to initial marking. The formation of gullies occurred due to further weathering and erosion by runoff water. This pointed towards the importance of a drainage system to ensure the stability of the slope. The runoff was drained out by the drain hole provided at the toe side of the slope to ensure no ponding condition. This effect is shown in Fig. 9c. With rainfall of 80 mm, water infiltrating through the cracks and the pores leads to the development of positive pore pressure by accumulating water between the soil layers. The friction resistance on the interface was reduced, resulting in the development of fracture along the sliding surface, resulting in a landslide as in Fig. 9d.

In previous studies, extensive researches show that the intermittent, low intensity, and shorter duration rainfall may help in stabilization of slope up to a certain extent by the development of negative pore pressure between the soil pores (Lee et al. 2014; Kristo et al. 2017). The threshold has been defined for the particular slope as the study is site specific which do not represent the threshold for all the landslides.

As the considered slope is recurring and may undergo failure in the future as the study proves that the slope is unstable under heavy rainfall condition and the area receives high-intensity rainfall during monsoonal season, thus, the threshold for the particular slope has been determined for the critical events seen during the physical model experiment for warning purposes.

This study was done to analyze the failure mechanism under the sudden and heavy rainfall condition by choosing an intensity of 30 mm/h as the region receives high-intensity rainfall during monsoonal seasons. To minimize the error while calculating the rainfall depth with intensity and time variation the rainfall was delivered in terms of depth of 10 mm by fixing the volume of water in the supply tank. To deliver 10 mm rainfall on the slope at 30 mm/h intensity, it took 20 min time. For proper infiltration, there is a gap is introduced between two consecutive rainfalls.

The first critical event occurred at 30 mm rainfall depth at which weathering and soil erosion starts due to heavy runoff and can be named as lower limit of warning threshold. The second critical event occurred at 50 mm rainfall depth at which rapid erosion and formation of erosional gullies can be seen which may help the water to infiltrate to much deeper extent even at higher intensity rainfall leading to the landslide initiation and can be named as upper limit of warning threshold. After delivering 80mm depth of rainfall the slope failure occurred and that can be named as failure

threshold for the particular slope, further number of physical modellings can be done to get the threshold for various landslides to generate the regional threshold for warning and prediction.

Numerical modelling test result

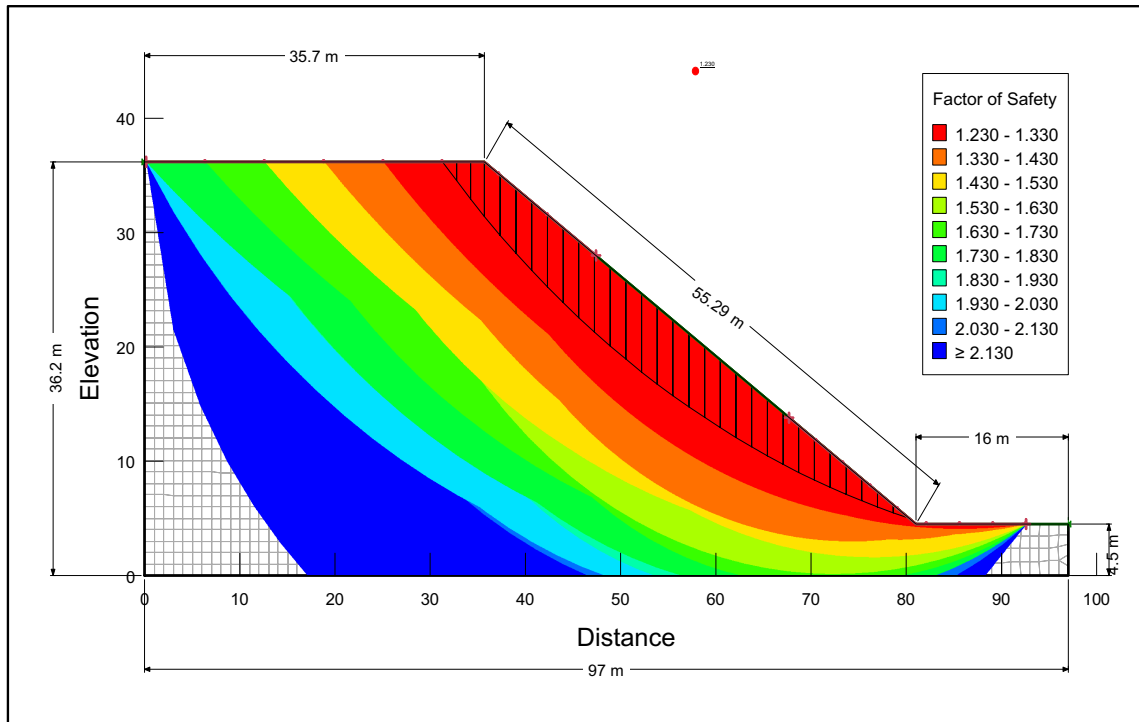
GeoStudio 2020 software has been used to simulate 2D rainfall in SEEP/W, which is directly linked to SLOPE/W for the analysis of slope stability, in order to investigate the failure pattern of the physical model. Using GeoStudio 2020 SLOPE/W stability software, this study performs a Morgenstern-Price method assessment of the soil slope's stability. The factor of safety was calculated using Morgenstern Price (Morgenstern and Price 1967) from the various limit equilibrium methods. It is one of the most widely used methods. It allows for a special variable interslice force function to be used, allowing the interslice inclination to vary on every slice along the slip surface while also satisfying both force and moment equilibrium. The geometry and material properties (cohesion, friction angle, and unit weight) of the slope are taken according to the model test as mentioned in the laboratory result section.

SLOPE/W results before the rainfall

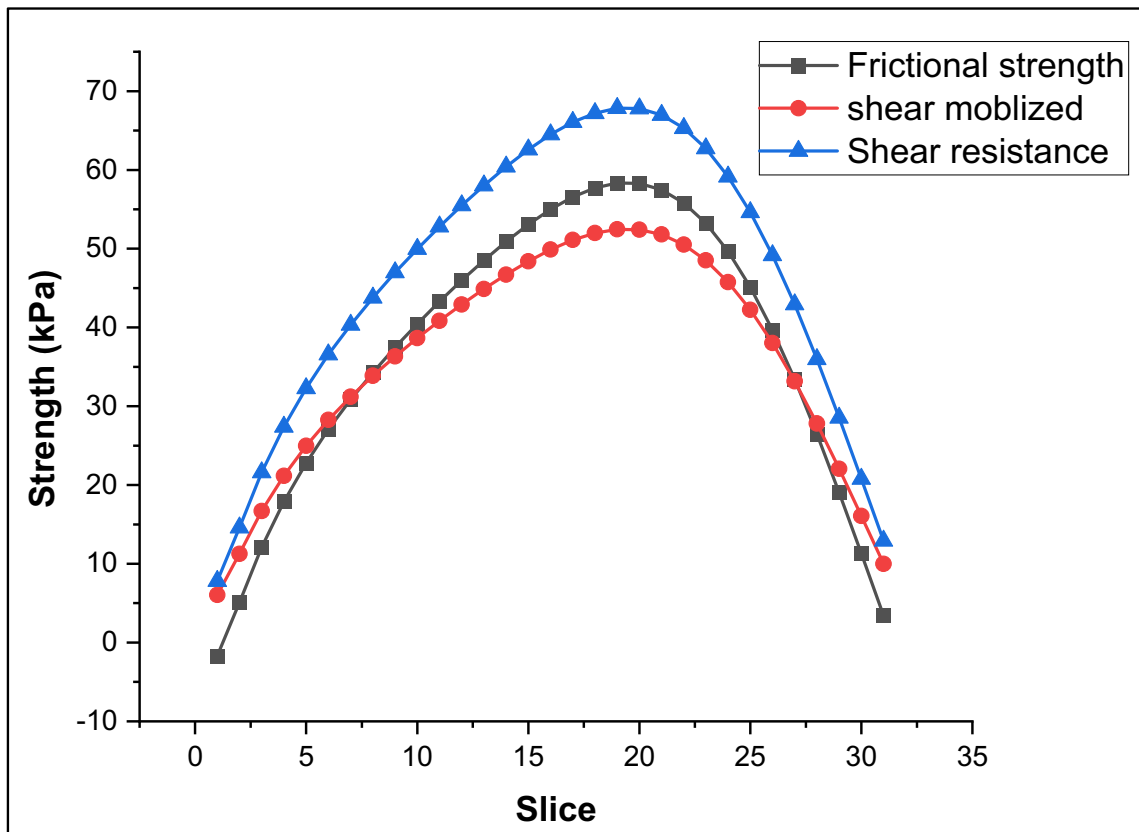
Slope stability analysis has been done to determine the factor of safety of the slope before the rainfall using soil parameters. Using the GeoStudio software, the factor of safety comes out to 1.23, which represents that the slope is very much stable on its own before the rainfall as the FOS of the slope is greater than 1. The critical slip failure pattern has been highlighted in Fig. 10a, which can fail under certain circumstances. It also represents the hazard zonation map according to the factor of safety. Figure 10b shows the relationship between friction strength, shear resistance, and shear mobilization. As shear resistance is much more excellent than the mobilized shear, which directly indicates, the slope is stable.

SEEP/W results after the rainfall

Rainfall simulation has been done in SEEP/W software under steady-state to analyze the effect of rainfall on the slope. The analysis gives a result of pore water pressure developed under the effect of desired rainfall intensity for the particular slope. The rainfall intensity was fixed to 30 mm/h according to the physical modelling experiment, and the rainfall boundary condition is used as a data point function in which the time duration has been fixed to 20 min to simulate the 10 mm rainfall depth for the 30 mm/h rainfall intensity. The bottom and left side of the geometry model has been set to impervious as a rock bed so that is there

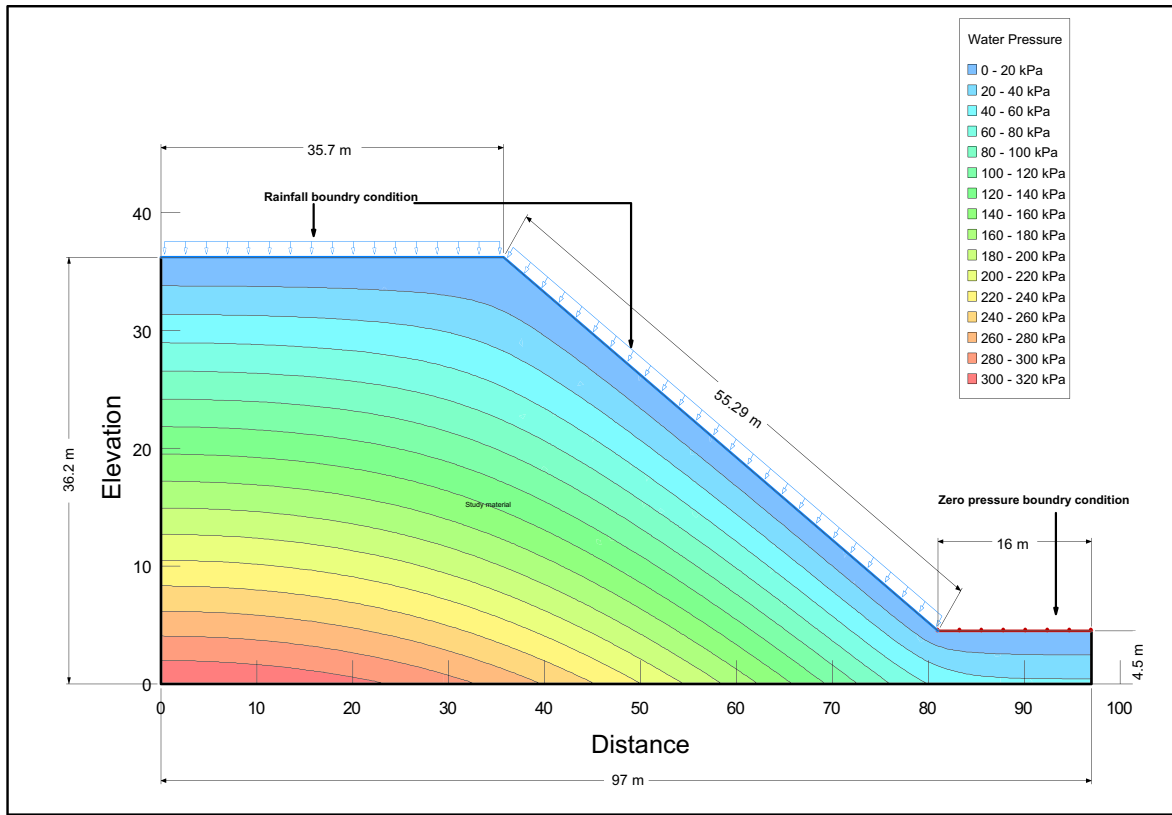


(a)

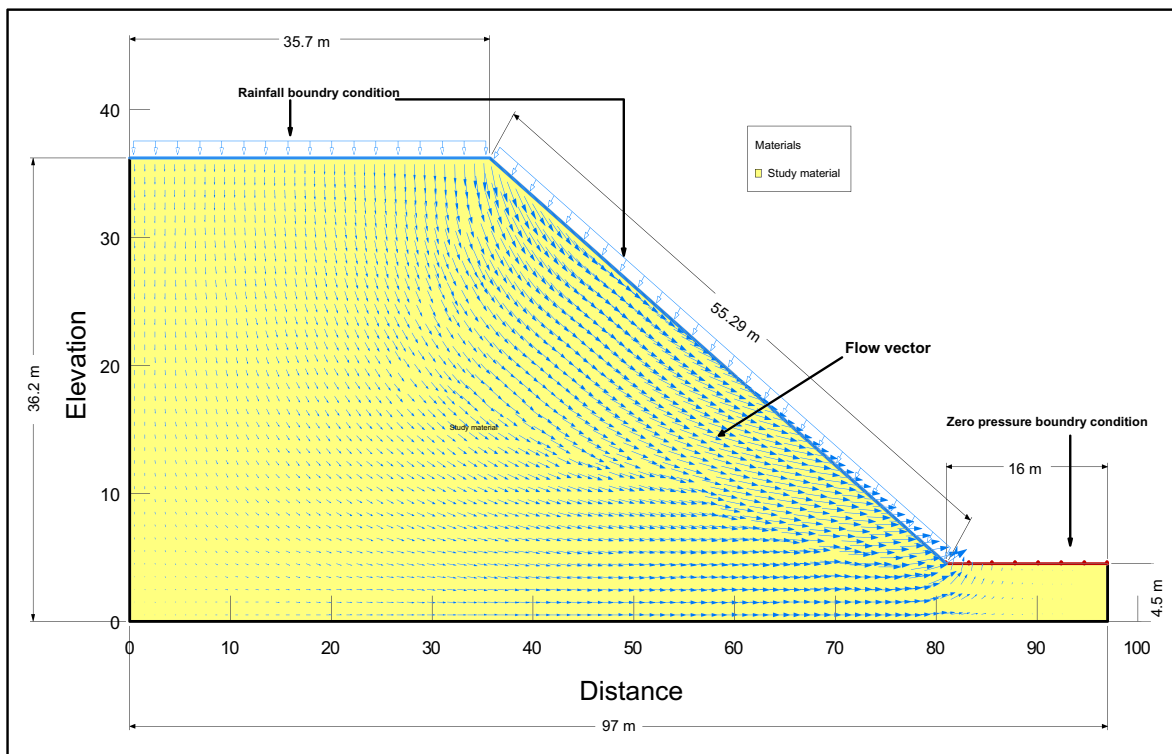


(b)

Fig. 10 a Stability analysis of slope before rainfall and b variation of shear strength, mobilized shears, and shear resistance before rainfall



(a)



(b)

Fig. 11 a Pore-pressure variation by rainfall and b flow vectors showing the flow direction of rainfall water

is no seepage can occur. The toe boundary condition has been set to zero pressure boundary condition, representing the drain path for the seepage water. Figure 11a represents the pore water pressure distribution according to depth. Figure 11b shows the flow vectors, which represent the direction of seepage flow. These figures also represent that the soil is fully saturated with the rainfall.

SLOPE/W results after the rainfall

Rainfall simulation done in SEEP/W is directly linked to SLOPE/W to analyze slope stability so that factor of safety can be determined after the rainfall, which will further help in monitoring and early warning. The safety factor comes out to be 0.626, which represents that the slope is very much critical to fail after the rainfall as the FOS of the slope is less than 1. The critical slip failure pattern has been highlighted in Fig. 12a, which failed under the action of rainfall. It also represents the hazard zonation map according to the factor of safety after the rain. Figure 12b shows the relationship between friction strength, shear resistance, and shear mobilized. As shear resistance is much lower than the mobilized shear, it indicates that the slope is unstable under the rainfall condition.

The numerical modelling result for the factor of safety of the slope before the rainfall was 1.23, and after the rainfall of desired intensity, it decreased to 0.626, which is less than 1, which justifies the physical modelling mechanism of failure for desired rainfall performed in the laboratory.

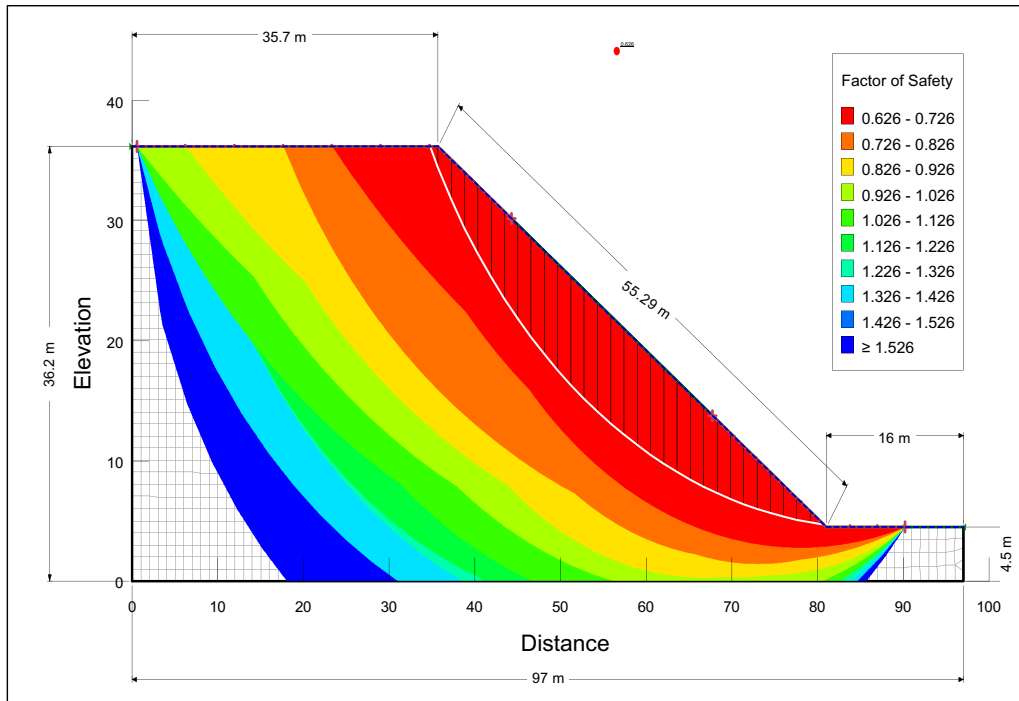
Discussion

In previous studies, only a few researchers (Askarinejad, et al., 2012; Li et al. 2016) studied rainfall-induced slope failure mechanisms using the physical modelling method. Li et al. (2016) concluded that the physical modelling method is very efficient to visualize the rainfall-induced landslides for a specific study area by performing the laboratory modelling test. It is tough to analyze it only by the mathematical or numerical model. Still, they did not perform numerical analysis to compare the results for validation purposes. So, to study the failure mechanism of a slope in the Himalayan region, a self-designed experimental platform has been developed to perform the physical model test on rainfall-induced landslides. The experimental platform includes an artificial rainfall generator, a loading mechanism, and a frame type box for modeling slope. The slope material has been made in the laboratory by similar material theory as it was not possible to take that much material from the site to the laboratory. The intensity for the rainfall generator was fixed to 30 mm/h. Each time, 10 mm rainfall is delivered to the slope to decrease the error while calculating the

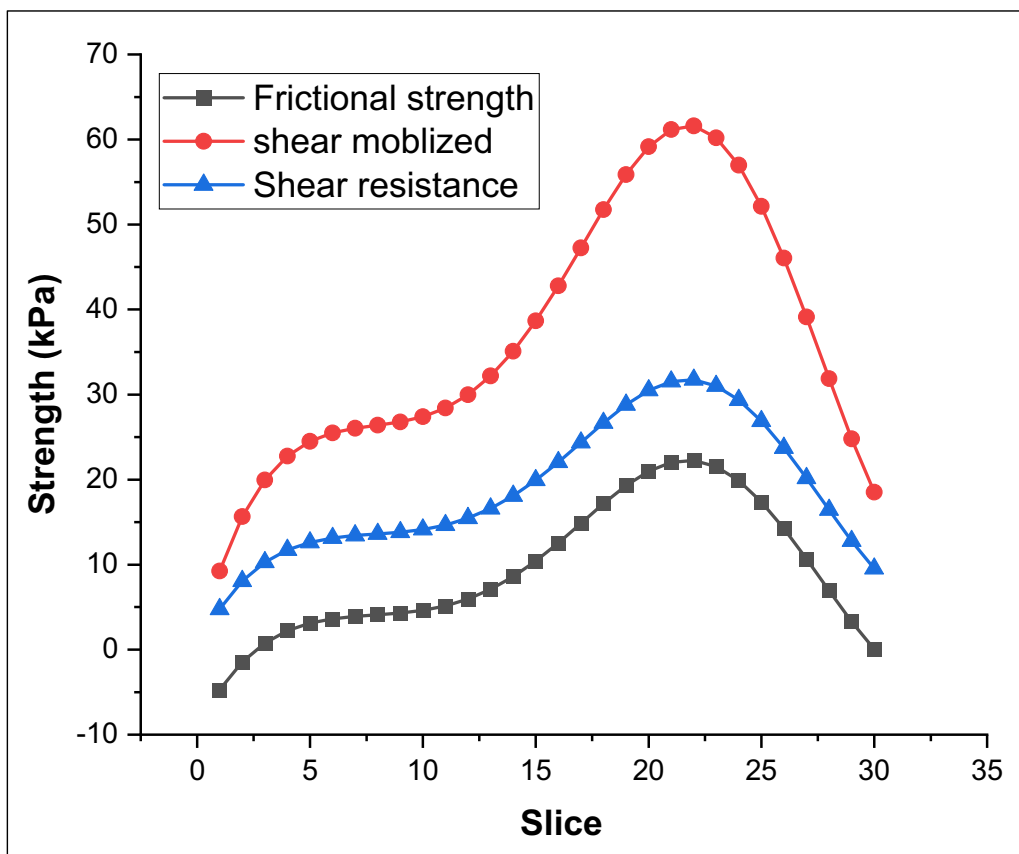
threshold for intensity duration relationship. The threshold has been determined as the total depth of rainfall till the failure for the particular slope. The physical model experiment using semi-similar material revealed a highly efficient way to visualize the pore water penetration process. The sliding mechanisms of the slope were studied, indicating that rainfall was the key factor before the slope failure. Many researchers proposed sliding mechanisms through various studies (Dahal 2012; Yang et al. 2015; Gupta et al. 2016; Senthilkumar et al. 2017), and from this study, the mechanism of slope failure is proposed.

The rapid sliding failure occurred at 80 mm rainfall depth, proposing the threshold value for the particular slope. However, weathering failure starts at 30 mm, which can be considered the warning threshold. As heavy rainfall occurs, water infiltrates into the soil layer and creates water levels between the slopes, increasing pore water pressure. The soil layer within the lower part will become fully saturated first because the thickness of the soil layer at the toe side is significantly less. As the hydraulic conductivity (k) of the soil is significantly less than rainfall intensity, most of the rainfall converts into surface runoff, which leads to the erosion of the slope's surface. This stage starts at 30 mm rainfall depth. Furthermore, in an increase in rainfall depth, i.e., at 50 mm rainfall depth, soil surface erosion increases rapidly, and formation of gullies can be seen on the slope, considered the initiation of slope failure, which can be regarded as extreme warning threshold and the restriction must be applied for any movement nearby the slope. Again, continuous increase in rainfall depth vigorous erosion may occur, which results in removal of the soil in the lower part of the slope, which provides the frictional resistance to the slope stability. Furthermore, the water level between the layers keeps increasing due to the continuous rainfall and infiltration, i.e., the pore water pressure in the soil keeps rising. After reaching a critical stage, sliding failure occurs. When the pore-water pressure crosses the limiting value, a shallow landslide is triggered by heavy rainfall. This stage occurred at 80 mm rainfall depth, and the safety factor is found significantly less.

Although many studies have been performed on numerical analysis (Acharya et al. 2016; Singh et al., 2018; Lin and Zhong 2019; Luo et al. 2021; Zhao 2021), they also lack validation with physical modelling results, as the behavior of landslide-causing factor may change with different location which needs validation. Therefore, seepage and slope stability simulations were performed using GeoStudio (2020) to check the feasibility of numerical modeling in the case of rainfall-induced landslides and compare and validate the results. Figure 10a shows the factor of safety for possible slip failure surfaces before the rainfall. The factor of safety before the rainfall was 1.23, which is greater than one and thus proves to be stable, and so does the physical model slope. Figure 10b shows the variation of shear strength,



(a)



(b)

Fig. 12 a Stability analysis of slope after rainfall and b variation of shear strength, mobilized shears, and shear resistance after rainfall

mobilized shear, and shear resistance, and clearly defines that the values of shear resistance are greater than the mobilized shear, which clearly defines the stability of slope before rainfall. In seepage simulation, the same rainfall intensity and duration is adopted as physical experiment condition. Figure 11a shows the pore water pressure distribution after the rainfall showing the infiltration of water in the soil pore, which acts as the primary initiative factor for slope failure. The same can be seen in the physical modelling result. Figure 12a shows the factor of safety contours after the rainfall. For critical slip, the surface factor of safety was 0.626, which is less than 1, proving the instability of the slope under the action of rainfall. Figure 12b shows that the mobilized shear becomes very high than the shear and friction resistance leading to the slope failure.

The physical and numerical modelling results verify that the rainfall infiltration due to the considered rainfall was responsible for slope failure. The methodology adopted in the study proves to be valid and can be used to simulate slope instability in the Himalayan region for further research.

There are some limitations of the study and supposed to be improved in the future research. It was impossible to transport so much material from the site to the laboratory for the experiment; there were certain assumptions and limitations in material modelling. As a result, there may be a risk of material similarity inaccuracy. The intensity of the rainfall was consistent throughout the experiment; however, in the actual condition, it is variable and cannot be anticipated precisely; thus, a constant intensity is assumed for the experiment. There would be some errors while taking the analysis of the results. As this investigation was undertaken to visualize the failure mechanism, one of the constraints was that no sensor was employed. Future studies may go further while addressing the study's shortcomings. The investigation was carried out to determine the rainfall threshold value for a particular slope. In case of failure triggered debris flow, the area of failure is usually much smaller than the actual affected area, and it is located somewhere upslope. The failed mass moves downward in the saturated condition and erodes the bed material, thereby increasing the volume of flow. Thus, the assumption made in this study that the slope fails in a single layer with circular failure can be a major limitation of the study. Moreover, the physical modelling experiment's threshold value was used in numerical modelling to validate the outcome, which was in close agreement with the physical modelling results.

Conclusion

The self-designed frame-type landslide model has been developed to include an experimental platform system and a self-made artificial rainfall system. The present study

results show that the methods used are a low-cost and effective method to monitor the infiltration process of water and landslides. The main triggering factor for shallow landslides is the high-intensity rainfall which generates heavy runoff water. Because of the heavy runoff water, soil erosion occurs, which helps initiate slope failures, and further rainfall continuity turned into a landslide. There were no arrangements for deformation, although by considering the scale effect the displacements and debris volume can be correlated up to some extent.

Based on lab studies, a high-intensity threshold of landslide numerical modelling has been done to justify the result. It is not possible to perform physical modelling experiments for all the cases. So numerical simulation for study areas has been completed, and the effects of numerical simulation and physical modelling are compared. It has been observed that numerical simulation is in close agreement with physical simulation. Hence in the future, numerical solutions can be easily used after selecting the proper parameter for finding out the threshold value of rainfall intensity which will cause landslides at the particular location. This threshold value can be used as a warning system for landslides for that specific slope. The present study provides scientific and theoretical guidance for early warning and monitoring for the rainfall-induced landslide. It provokes researchers to move forward in this field by minimizing the limitation of this study.

Acknowledgements The authors are thankful to the Delhi Technological University for providing the research facilities and funding to support this study.

Data Availability All data, models, or codes that support the findings of this study are available from the corresponding author upon reasonable request.

Declarations

Conflict of interest The authors declare that they have no competing interests.

References

- Abraham MT, Satyam N, Pradhan B, Alamri AM (2020a) Forecasting of landslides using rainfall severity and soil wetness: a probabilistic approach for Darjeeling Himalayas. *Water (switzerland)* 12:1–19. <https://doi.org/10.3390/w12030804>
- Abraham MT, Satyam N, Reddy SKP, Pradhan B (2021) Runout modeling and calibration of friction parameters of Kurichermala debris flow, India. *Landslides* 18:737–754. <https://doi.org/10.1007/s10346-020-01540-1>
- Abraham MT, Satyam N, Pradhan B et al (2022) Developing a prototype landslide early warning system for Darjeeling Himalayas using SIGMA model and field based monitoring. *Geosci J* 26:289–301. <https://doi.org/10.1007/s12303-021-0026-2>
- Abraham MT, Satyam N, Pradhan B, Alamri AM (2020b) Iot-based geotechnical monitoring of unstable slopes for landslide early

- warning in the Darjeeling Himalayas. *Sensors* (Switzerland) 20. <https://doi.org/10.3390/s20092611>
- Abraham MT, Satyam N, Rosi A, et al (2020c) The Selection of rain gauges and rainfall parameters in estimating intensity-duration thresholds for landslide occurrence: case study from Wayanad (India). *Water* (Switzerland) 12. <https://doi.org/10.3390/W12041000>
- Acharya KP, Bhandary NP, Dahal RK, Yatabe R (2016) Seepage and slope stability modelling of rainfall-induced slope failures in topographic hollows. *Geomatics, Nat Hazards Risk* 7:721–746. <https://doi.org/10.1080/19475705.2014.954150>
- Askarinejad A, Laue J, Zweidler A, et al (2012) Physical modelling of rainfall induced landslides under controlled climatic conditions. *Eurofuge* 2012
- BIS:2720 (Part 1) (2006) Indian standard methods of test for soils : preparation of dry soil samples for various tests. *Bur Indian Stand New Delhi*
- Cai G, Li M, Han B, et al (2020) Numerical analysis of unsaturated soil slopes under rainfall infiltration based on the modified glasgow coupled model. *Adv Civ Eng* 2020. <https://doi.org/10.1155/2020/8865179>
- Collins BD, Znidarcic D (2004) Stability analyses of rainfall induced landslides. *J Geotech Geoenvironmental Eng* 130:362–372. [https://doi.org/10.1061/\(asce\)1090-0241\(2004\)130:4\(362\)](https://doi.org/10.1061/(asce)1090-0241(2004)130:4(362))
- Dahal RK (2012) Rainfall-induced landslides in Nepal. *Int J Eros Control Eng* 5:1–8. <https://doi.org/10.13101/ijece.5.1>
- Dikshit A, Sarkar R, Satyam N (2018) Probabilistic approach toward Darjeeling Himalayas landslides-A case study. *Cogent Eng* 5:1–11. <https://doi.org/10.1080/23311916.2018.1537539>
- Dikshit A, Satyam N, Pradhan B, Kushal S (2020b) Estimating rainfall threshold and temporal probability for landslide occurrences in Darjeeling Himalayas. *Geosci J* 24:225–233. <https://doi.org/10.1007/s12303-020-0001-3>
- Dikshit A, Sarkar R, Pradhan B, et al (2020a) Rainfall induced landslide studies in Indian Himalayan region: a critical review. *Appl Sci* 10. <https://doi.org/10.3390/app10072466>
- Fredlund DG, Xing A (1994) Equations for the soil-water characteristics curve. *Can Geotech J*. 31:533–546
- Geo-Slope (2012a) Stability modeling with Slope/W, Geo-Slope International Ltd. Canada
- Geo-Slope (2012b) Seepage Modeling with SEEP/W 2015. *Geostudio Help-file*. <http://www.geo-slope.com>
- Geo-Slope (2012c) Seep/W generated pore-water pressures in Slope/W stability analysis, Geo-Slope International Ltd. Canada
- Godt JW, Baum RL, Lu N (2009) Landsliding in partially saturated materials. *Geophys Res Lett* 36. <https://doi.org/10.1029/2008GL035996>
- Gupta V, Bhasin RK, Kaynia AM et al (2016) Landslide Hazard in the Nainital township, Kumaun Himalaya, India: the case of September 2014 Balia Nala landslide. *Nat Hazards* 80:863–877. <https://doi.org/10.1007/s11069-015-2002-5>
- Guzzetti F, Peruccacci S, Rossi M, Stark CP (2008) The rainfall intensity-duration control of shallow landslides and debris flows: An update. *Landslides* 5:3–17. <https://doi.org/10.1007/s10346-007-0112-1>
- Harris SJ, Orense RP, Itoh K (2012) Back analyses of rainfall-induced slope failure in Northland Allochthon formation. *Landslides* 9:349–356. <https://doi.org/10.1007/s10346-011-0309-1>
- Hopkins TC, Allen DL, Deen RC (1975) Effects of Water on Slope Stability. 45p
- HPSDMA (2009) District Survey Document Shimla. 1–23
- IS 14496 (Part 2): 1998 (2007) Preparation of landslide hazard zonation maps in mountainous terrains - guidelines part 2 macrozonation. Bureau of Indian Standards, New Delhi, India
- IS:2720 (Part 3):1980 (1980) Indian Standard, Determination of specific gravity, Part 3 (Section II)- Fine, medium and coarse grained soils. Bureau of Indian Standards, New Delhi, India
- IS: 2720 (part 12) (1981) Determination of shear strength parameters of soil from consolidated undrained triaxial compression test with measurement of pore water pressure. IS:2720 Part XII, Bureau of Indian Standards, New Delhi, India
- IS: 2720 (part 17) (1987) Laboratory determination of permeability. Bureau of Indian Standards, New Delhi, India Reaffirmed: 54:273–276
- IS: 2720 (part 5) (1985) Indian Standard, Methods of test for soils, Part 5: Determination of liquid limit and plastic limit. Bureau of Indian Standards, New Delhi, India Reaffirmed:1–16
- IS: 2720 (part 7) (2011) Methods of test for soils, determination of water content dry density relation using light compaction. IS:2720 (Part VII-1980), Bureau of Indian Standards, New Delhi, India Reaffirmed:1–16
- IS: 2720 (part 8) (1983) Determination of water content-dry density relation using heavy compaction. IS:2720 Part VIII, Bureau of Indian Standards, New Delhi, India Reaffirmed:3562–3577
- IS:2720 (Part 2) (1973) Indian standard, Methods of test for soils, Part 2: Determination of water content. Bureau of Indian Standards, New Delhi, India
- IS:2720 (Part 4):1985 (1985) Indian Standard, Methods of Test for Soils, Part 4: Grain size analysis. Bureau of Indian Standards, New Delhi, India
- Iverson RM (2000) Landslide triggering by rain infiltration. *Water Resour Res* 36:1897–1910. <https://doi.org/10.1029/2000WR900090>
- Jagodnik V (2019) Rainfall infiltration and stability analysis of an unsaturated slope in residual soil from flysch rock mass Infiltration pluviale et analyse de la stabilité d'une pente non saturée. <https://doi.org/10.32075/17ECMGE-2019-0906>
- Jeong S, Lee K, Kim J, Kim Y (2017) Analysis of rainfall-induced landslide on unsaturated soil slopes. *Sustain* 9:1–20. <https://doi.org/10.3390/su9071280>
- Josifovski J, Susinob V, Tasevska M (2019) Experimental and Numerical Modelling of Rainfall Induced Slope
- Kanungo DP, Sharma S (2014) Rainfall thresholds for prediction of shallow landslides around Chamoli-Joshimath region, Garhwal Himalayas, India. *Landslides* 11:629–638. <https://doi.org/10.1007/s10346-013-0438-9>
- Kristo C, Rahardjo H, Satyanaga A (2017) Effect of variations in rainfall intensity on slope stability in Singapore. *Int Soil Water Conserv Res* 5:258–264. <https://doi.org/10.1016/j.iswcr.2017.07.001>
- Kuriakose SL, Sankar G, Muraleedharan C (2009) History of landslide susceptibility and a chorology of landslide-prone areas in the Western Ghats of Kerala, India. *Environ Geol* 57:1553–1568. <https://doi.org/10.1007/s00254-008-1431-9>
- Lee ML, Ng KY, Huang YF, Li WC (2014) Rainfall-induced landslides in Hulu Kelang area, Malaysia. *Nat Hazards* 70:353–375. <https://doi.org/10.1007/s11069-013-0814-8>
- Li C, Yao D, Wang Z et al (2016) Model test on rainfall-induced loess-mudstone interfacial landslides in Qingshuihe, China. *Environ Earth Sci* 75:1–18. <https://doi.org/10.1007/s12665-016-5658-6>
- Lin H, Zhong W (2019) Influence of rainfall intensity and its pattern on the stability of unsaturated soil slope. *Geotech Geol Eng* 37:615–623. <https://doi.org/10.1007/s10706-018-0631-7>
- Luo Y, He S ming, Chen F zhu, et al (2015) A physical model considered the effect of overland water flow on rainfall-induced shallow landslides. *Geoenvironmental Disasters* 2. <https://doi.org/10.1186/s40677-015-0017-6>
- Luo X, Yuan J, Gu T (2021) Study on the stability of slopes on both sides of highway in rock area under rainfall. *Arab J Geosci* 14. <https://doi.org/10.1007/s12517-021-06857-2>

- Matziaris V, Marshall AM, Heron CM, Yu HS (2015) Centrifuge model study of thresholds for rainfall-induced landslides in sandy slopes. *IOP Conf Ser Earth Environ Sci* 26. <https://doi.org/10.1088/1755-1315/26/1/012032>
- Morgenstern NR, Price VE (1967) A numerical method for solving the equations of stability of general slip surfaces. *Comput J* 9:388–393. <https://doi.org/10.1093/comjnl/9.4.388>
- Panchal S, Shrivastava AK (2021) A comparative study of frequency ratio, Shannon's entropy and analytic hierarchy process (Ahp) models for landslide susceptibility assessment. *ISPRS Int J Geo-Information* 10. <https://doi.org/10.3390/ijgi10090603>
- Panchal S, Shrivastava AK (2022) Landslide hazard assessment using analytic hierarchy process (AHP): a case study of National Highway 5 in India. *Ain Shams Eng J* 13:101626. <https://doi.org/10.1016/j.asej.2021.10.021>
- Parkash S (2011) Historical records of socio-economically significant landslides in India. *South Asia Disaster Stud* 4:177–204
- Paswan AP, Shrivastava AK (2022a) Stability analysis of rainfall-induced landslide. In: 3rd International Online Conference on Emerging Trends in Multi-Disciplinary Research "ETMDR-2022a." pp 505–509, ISBN: 9789355935243
- Paswan AP, Shrivastava AK (2022b) Numerical modelling of rainfall-induced landslide. In: International e-Conference on Sustainable Development & Recent Trends in Civil Engineering. pp 8–13, ISBN: 9789355934314
- Peres DJ, Cancelliere A, Greco R, Bogaard TA (2018) Influence of uncertain identification of triggering rainfall on the assessment of landslide early warning thresholds. *Nat Hazards Earth Syst Sci* 18:633–646. <https://doi.org/10.5194/nhess-18-633-2018>
- Senthilkumar V, Chandrasekaran SS, Maji VB (2017) Geotechnical characterization and analysis of rainfall-induced 2009 landslide at Marappalam area of Nilgiris district, Tamil Nadu state, India. *Landslides* 14:1803–1814. <https://doi.org/10.1007/s10346-017-0839-2>
- Sharma RK, Mehta BS, Jamwal CS (2013) Cut slope stability evaluation of NH-21 along Nalayan-Gambhrola section, Bilaspur district, Himachal Pradesh, India. *Natural Hazards* 66:249–270. <https://doi.org/10.1007/s11069-012-0469-x>
- Singh AK, Kundu J, Sarkar K (2018) Stability analysis of a recurring soil slope failure along NH-5, Himachal Himalaya, India. *Nat Hazards* 90:863–885. <https://doi.org/10.1007/s11069-017-3076-z>
- Skempton AW (1985) Residual strength of clays in landslides, folded strata and the laboratory. *Geotechnique* 35:3–18. <https://doi.org/10.1680/geot.1985.35.1.3>
- Uchimura T, Towhata I, Wang L et al (2015) Precaution and early warning of surface failure of slopes using tilt sensors. *Soils Found* 55:1086–1099. <https://doi.org/10.1016/j.sandf.2015.09.010>
- Wieczorek GF (1996) Landslide Triggering Mechanisms. In: Turner AK, Schuster RL (eds) *Landslides: Investigation and Mitigation*. Transportation Research Board, National Research Council, Special Report, Washington, DC, pp 76–90
- Wong STY, Ong DEL, Robinson RG (2017) Behaviour of MH silts with varying plasticity indices. *Geotech Res* 4:118–135. <https://doi.org/10.1680/jgere.17.00002>
- Xie Q, Cao Z, Xie W et al (2021) Model test and numerical analysis of cutting slope with skip cut method. *Nat Hazards Rev* 22:04021002. [https://doi.org/10.1061/\(asce\)nh.1527-6996.0000448](https://doi.org/10.1061/(asce)nh.1527-6996.0000448)
- Yang H, Wang F, Vilímek V, et al (2015) Investigation of rainfall-induced shallow landslides on the northeastern rim of Aso caldera, Japan, in July 2012. *Geoenvironmental Disasters* 2. <https://doi.org/10.1186/s40677-015-0028-3>
- Zhang LL, Zhang J, Zhang LM, Tang WH (2011) Stability analysis of rainfall-induced slope failure: a review. *Proc Inst Civ Eng Geotech Eng* 164:299–316. <https://doi.org/10.1680/geng.2011.164.5.299>
- Zhang L, Wu F, Zhang H et al (2019) Influences of internal erosion on infiltration and slope stability. *Bull Eng Geol Environ* 78:1815–1827. <https://doi.org/10.1007/s10064-017-1185-2>
- Zhao Y (2021) Transient stability analysis method and sensitivity study of unsaturated soil slopes under consideration of rainfall conditions. *Arab J Geosci* 14. <https://doi.org/10.1007/s12517-021-07514-4>